DISSOLUTION BEHAVIOUR OF COPPER AND NICKEL OXIDES IN MOLTEN $Li_2CO_3/Na_2CO_3/K_2CO_3$

YASUHIKO ITO, KIYOSHI TSURU and JUN OISHI

Department of Nuclear Engineering, Faculty of Engineering, Kyoto University, Sakyo-ku, Kyoto 606 (Japan)

YOSHINORI MIYAZAKI and TERUO KODAMA

Fuel Cell Section, Government Industrial Research Institute, Osaka, Midorigaoka 1-8-31, Ikeda, Osaka 563 (Japan)

(Received August 31, 1987; in revised form November 13, 1987)

Summary

An $Li_2CO_3/Na_2CO_3/K_2CO_3$ eutectic melt has been taken as a typical example of a molten carbonate system, and the dissolution behaviour of the oxides of nickel and copper in the melt have been investigated at 873 K. The solubility products of CuO and NiO in the melt have been estimated to be 8.9×10^{-9} mol^2 l^{-2} and $3.8(\pm 0.6) \times 10^{-10}$ mol^2 l^{-2}, respectively. The diffusion coefficients of Cu(II) and Ni(II) ions in the melt are approximately 7.2×10^{-5} cm^2 s^{-1} and $2.2(\pm 0.5) \times 10^{-5}$ cm^2 s^{-1}, respectively. When the oxide-ion concentration in the melt is high, two new peaks are observed in the voltammogram for CuO. These peaks have been attributed to the direct electrochemical reduction of particles of CuO and Cu_2O.

Introduction

Molten carbonates are promising materials for application in many future energy processes, such as molten-carbonate fuel cells (MCFCs), thermal energy storage, nuclear waste processing, coal gasification, etc. [1, 2]. The development of MCFCs is attracting particular attention at the present time, but there are still many technological problems to be solved. For example, achieving a good corrosion resistance for both the electrode and the cell construction materials is an especially important problem to be overcome. In order to gain a quantitative understanding of the corrosion processes, it is necessary to determine the behaviour of the oxide-ion in the melt. To this end, the authors have used [3] a stabilized zirconia–air electrode as an oxide-ion indicator and have demonstrated its suitability in an $Li_2CO_3/Na_2CO_3/K_2CO_3$ eutectic melt. In particular, the electrode has been employed to determine the dissociation constant of the reaction:

0378-7753/88/$3.50

$$CO_3^{2-}(l) = CO_2(g) + O^{2-}(l) \quad (1)$$

In the work reported here, and drawing upon results obtained in a previous study [3], the dissolution behaviour of the oxides of nickel and copper have been investigated in detail, using a potential-sweep method and several conventional analytical techniques. In addition, studies of the direct electrochemical reduction of metal oxides on the cathode are discussed. Nickel is a major component of MCFC anode material, and nickel oxide is used as a cathode material. On account of its favourable economics, copper is also considered to be a suitable anode material.

Experimental

In studies on the solubility of metal oxides in molten carbonate systems, Baumgartner [4, 5] has reported results for NiO, CuO, ZnO, $LiFeO_2$, and $LaNiO_3$, while Ota *et al.* [6] have examined NiO. In both investigations, the concentration of saturated metallic ion was determined by atomic absorption spectroscopic analysis. In the work reported here, a different method has been applied to obtain the solubility data. That is, a potential sweep technique has been employed to determine the saturated concentration of the metallic ions, from which the solubility products have been derived using oxide-ion concentration data measured by a zirconia–air electrode.

The experimental cell is shown in Fig. 1. Commercial Li_2CO_3, Na_2CO_3 and K_2CO_3 (Reagent Grade, Wako Chemicals Co., Ltd.) were mixed together and the eutectic mixture (Li_2CO_3: 0.435, Na_2CO_3: 0.315, K_2CO_3: 0.250 mole fraction, melting point 670 K [7]) was then vacuum dried for 48 h at 473 K. The eutectic mixture was melted under a dry, carbon dioxide gas atmosphere and maintained at 873 K in a high-purity alumina crucible (Nippon Kagaku Togyo Co., Ltd., SSA-S). A gold wire (5 mm dia.) served

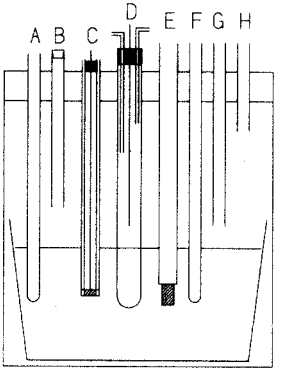

Fig. 1. Experimental cell. A, thermocouple; B, $CuCl_2$ inlet; C, working electrode; D, reference electrode ('oxygen electrode'); E, counter electrode; F, stabilized zirconia; G, gas inlet; H, gas outlet.

as a working disc electrode. The wire was located inside a high-purity alumina tube and fixed in position by alumina cement (Toa Gosei Kagaku Co., Ltd., Alonceramic-D). An 'oxygen electrode' (P_{O_2} = 33.8 kPa and P_{CO} = 67.5 kPa [7]) was used as a reference electrode. The counter electrode consisted of a glassy carbon rod. An yttria- or magnesia-stabilized zirconia tube (Nippon Kagaku Togyo Co., Ltd.) was employed as an indicator electrode for measuring the oxide-ion concentration. In order to determine the relationship between the peak current observed on the voltammogram and the concentration of metallic ion in the melt, it is necessary to control the latter closely. This was achieved by adding a known amount of metal chloride. The latter was prepared in a dry-box to avoid contamination. The effect of the chloride ion on the oxide-ion concentration measurement was assumed to be negligible. Where necessary, X-ray diffraction analysis of the electrode surface was also conducted.

Results and discussion

Measurement of solubility product

In order to determine the solubility product of CuO in the melt, voltammograms were obtained at several calculated (apparent) copper(II) chloride concentrations. A typical curve is shown in Fig. 2. It can be seen that a distinct cathodic current peak occurs at around —260 mV and an anodic current peak at around —60 mV. Note, potentials are given *versus* the 'oxygen electrode'. The peak current at —260 mV is dependent upon the amount of copper(II) chloride added to the melt. The sharp increase in the anodic current at around +80 mV is attributed to decomposition of the melt. Figure 3 shows the relationship between the cathode peak current and the square root of the scan rate, while Fig. 4 presents plots of this peak current

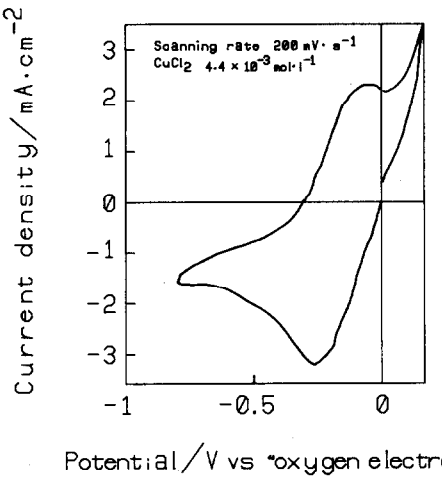

Fig. 2. Voltammogram for carbonate melt containing Cu(II).

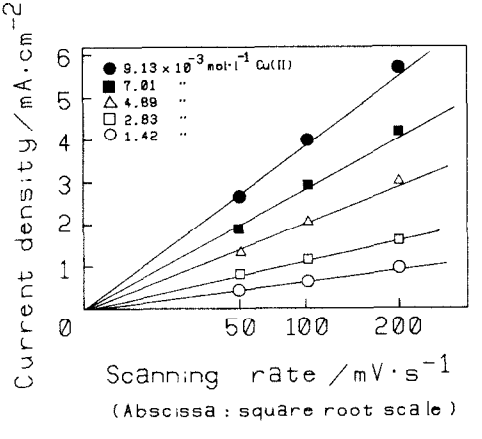

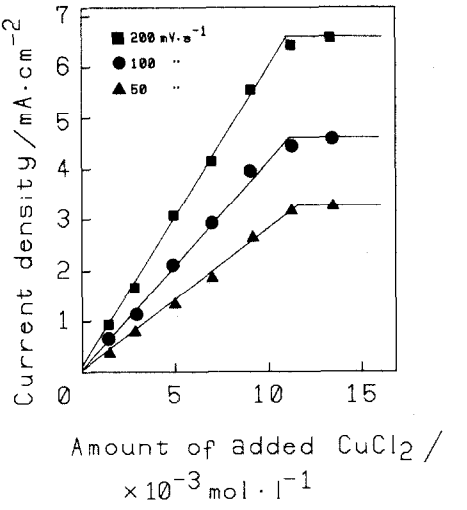

Fig. 3. Peak current *vs.* scan rate for carbonate melt containing Cu(II).

Fig. 4. Peak current *vs.* $CuCl_2$ addition for carbonate melt.

versus the concentration of copper(II) ion in the melt. Note, concentrations are given in terms of mol l^{-1}. At low concentrations, the cathodic peak current is directly proportional to both the square root of the scan rate and the copper(II) chloride concentration; this indicates that the reaction corresponding to the peak is diffusion controlled. On the other hand, as the amount of added copper(II) ion is increased, each peak-current relationship changes slope at the same concentration (Fig. 4). In other words, the concentration of copper(II) ion in the melt no longer increases despite the further addition of copper(II) chloride. Instead, copper(II) oxide starts to precipitate. The concentration at this stage is considered to be the saturated value of copper(II) ion under the carbon dioxide atmosphere, namely, 1.1×10^{-2} mol l^{-1}. In previous work [3], the oxide-ion concentration under a carbon dioxide atmosphere of 101 kPa was found to be 8.1×10^{-7} mol l^{-1}. It is therefore concluded that the solubility product of copper(II) oxide in the melt is 8.9×10^{-9} mol^2 l^{-1}.

By using data from Fig. 4, the diffusion coefficient of copper(II) ion in the melt is calculated to be:

$$D_{Cu(II)} = 7.2 \times 10^{-5} \text{ cm}^2 \text{ s}^{-1}$$

This determination is based on the well-known Nicholson equation [8], namely,

$$i_p = 0.4463 \times 10^{-3} n^{3/2} F^{3/2} (RT)^{-1/2} D_O^{1/2} C_O^* \nu^{1/2}$$

where: i_p is the peak current density; n is the number of electrons transferred; F is the Faraday constant; R is the gas constant; T is the temperature;

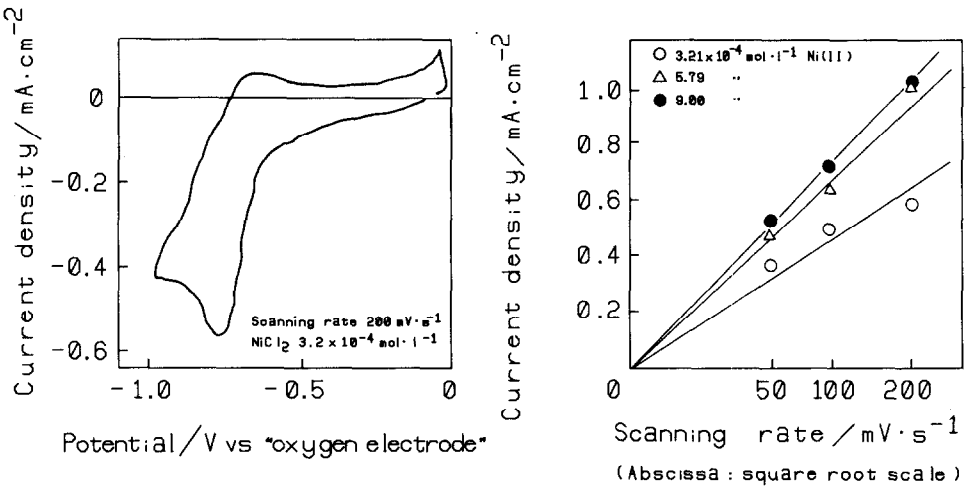

Fig. 5. Voltammogram for carbonate melt containing Ni(II).

Fig. 6. Peak current *vs.* scan rate for carbonate melt containing Ni(II).

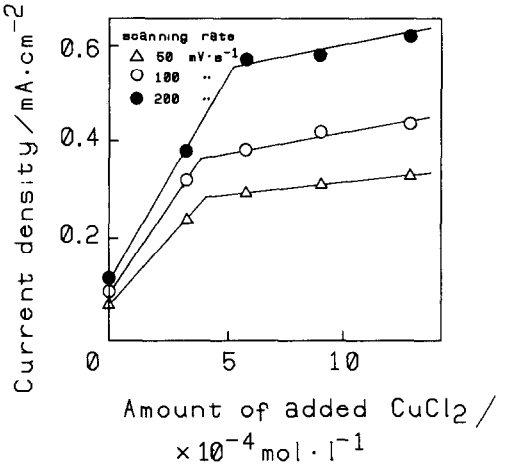

Fig. 7. Peak current *vs.* $NiCl_2$ addition for carbonate melt.

D_O and C_O^* are the diffusion coefficient and bulk concentration of the relevant species, respectively; and ν is the scan rate.

The same procedure has been applied to determine the solubility product of nickel(II) oxide. Figure 5 shows a typical voltammogram. A distinct cathodic peak is observed around —770 mV, while an anodic peak appears around —660 mV. Figure 6 demonstrates the relationship between the cathodic peak current and the square root of the scan rate, and Fig. 7 that between the cathodic peak current and the concentration of nickel(II) ion. The solubility product of nickel(II) oxide is significantly lower than that

of copper(II) oxide, and the point at which the slope changes in Fig. 7 (which indicates saturation of nickel ion) is not so clearly defined. Furthermore, because of residual current due to contaminants, a gradual increase in the peak current continues beyond this concentration point. For these reasons, it is not possible to make a precise measurement of the concentration of saturated nickel(II) ion; the estimated value is $4.7(\pm 0.7) \times 10^{-4}$ mol l^{-1}. Accordingly, by the same procedure described above, the solubility product of nickel(II) oxide is found to be approximately $3.8\ (\pm 0.6) \times 10^{-10}$ $mol^2\ l^{-1}$. In turn, the diffusion coefficient of nickel(II) ion in the melt is estimated to be:

$$D_{Ni(II)} = 2.2(\pm 0.5) \times 10^{-5}\ cm^2\ s^{-1}$$

Tumanova *et al.* [10] have reported values of 3.78×10^{-5} and 4.89×10^{-5} $cm^2\ s^{-1}$ for $D_{Cu(II)}$ and $D_{Ni(II)}$, respectively, in an Li_2CO_3–K_2CO_3 system at 913 K. These values are in fair agreement with those reported here. It should be noted, however, that the experiments of these authors were conducted under different conditions and the details of the experimental procedure are not clear.

Direct electrochemical reduction of metal oxide

The above experiments, designed to determine the concentration of saturated copper(II) ion in the melt, have revealed a further interesting phenomenon. That is, when copper(II) chloride is added so that the apparent (calculated) concentration of copper(II) chloride proceeds beyond the slope-changing point of Fig. 4, two new peak pairs appear in the voltammogram as shown in Fig. 8. These new peaks are present in both the cathodic and anodic scans. In order to understand the cause of this phenomenon, voltammograms have been obtained under several partial pressures of carbon dioxide gas. In Fig. 9, curves (a) and (b) are voltammograms obtained

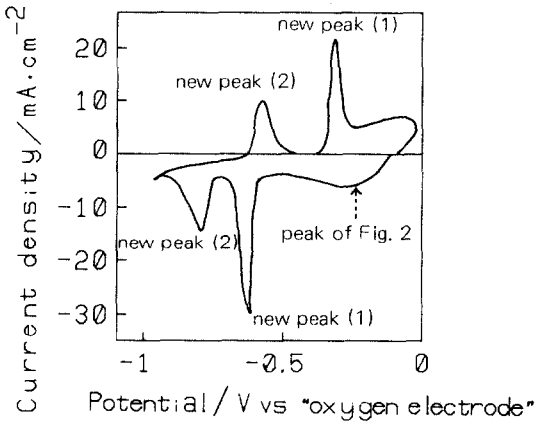

Fig. 8. Voltammogram for carbonate melt of high $CuCl_2$ content.

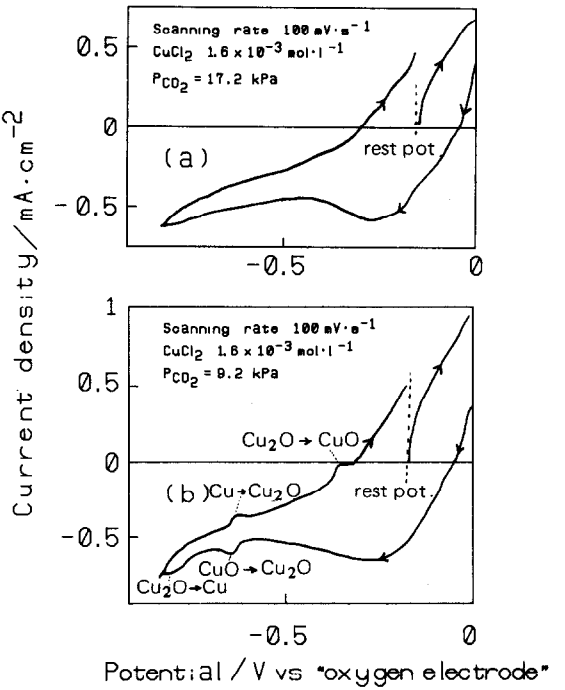

Fig. 9. Voltammograms for carbonate melt having high $CuCl_2$ content under CO_2 partial pressure of (a) 17.2 kPa; (b) 9.2 kPA.

under pressures of 17.2 kPa and 9.2 kPa, respectively. Comparison of the two curves reveals the existence of an additional peak in Fig. 9(b). Taking into consideration that this phenomenon occurs only at high oxide-ion concentrations, *i.e.*, at low CO_2 partial pressures, the appearance of the two peaks might be attributed to the formation of copper(II) oxide precipitates in the melt. From the above estimated value of the solubility product of copper(II) oxide, and given that the copper(II) ion concentration (calculated) in the melt was 1.6×10^{-3} mol l^{-1}, the critical partial pressure of CO_2 at which the melt is saturated with copper(II) oxide is calculated to be 15.2 kPa. Thus, when the partial pressure of CO_2 exceeds this value (*e.g.*, Fig. 9(a) where the pressure is 17.2 kPa), the melt is not saturated and the peak corresponding to the new peak in Fig. 8 is not observed. On the other hand, when the partial pressure of CO_2 is <15.2 kPa (*e.g.*, Fig. 9(b) where the pressure is 9.2 kPa), the new peak is observed. From these observations, the phenomenon can be attributed to the direct electrochemical reduction of the oxide particles. The same phenomenon can be observed in voltammograms obtained at other copper(II) chloride concentrations. X-ray diffraction analysis of the electrode surface after potentiostatic electrolysis shows that the two voltammetric peaks correspond, sequentially, to the reactions:

$$2CuO + 2e^- \longrightarrow Cu_2O + O^{2-} \quad (4)$$

and

$$Cu_2O + 2e^- \longrightarrow 2Cu + O^{2-} \quad (5)$$

Thus, in considering the metal transfer from cathode to anode through the electrolyte in an MCFC, besides the dissolution of the positive electrode (cathode) followed by a metal deposition near the anode, the direct electrochemical reduction of oxide particles coming from the cathode should also be taken into account.

Acknowledgement

This work has been carried out with support from the Japanese Ministry of Education, Science and Culture.

References

1 J. R. Selman and L. G. Marianowski, in D. G. Lovering (ed.), *Molten Salt Technology*, Plenum, New York, 1982, pp. 323 - 393.
2 J. R. Selman and H. C. Maru, in G. Mamantov and J. Braunstein (eds.), *Advances in Molten Salt Chemistry*, Vol. 4, Plenum, New York, 1981, pp. 159 - 390.
3 Y. Ito, K. Tsuru, J. Oishi, Y. Miyazaki and T. Kodama, *J. Power Sources, 16* (1985) 75.
4 C. E. Baumgartner, *J. Am. Ceram. Soc., 67* (1984) 460.
5 C. E. Baumgartner, *J. Electrochem. Soc., 131* (1984) 1850.
6 T. Shinjo, N. Kamiya and K. Ota, *Proc. 27th Battery Symp. Japan, Osaka, 1986*, pp. 225 - 226; K. Ota, T. Shinjo and N. Kamiya, *Denki Kagaku, 55* (1987) 323.
7 E. S. Argano and J. Levitan, *J. Electrochem. Soc., 116* (1969) 153.
8 R. S. Nicholson and I. Shain, *Anal. Chem., 36* (1964) 706.
9 G. J. Janz and M. R. Lorenz, *J. Chem. Eng. Data, 6* (1961) 321.
10 N. K. Tumanova and Yu. K. Delimarskii, *Ukr. Khim. Zh., 30* (1964) 682.